GEODEZJA I KARTOGRAFIA
GEODESY AND CARTOGRAPHY
Vol. 54, No 2, 2005, pp. 51-68

Density and Gravity Interpolation Effects on Helmert Geoid Determination

Sujan Bajracharya, Michael G. Sideris

Department of Geomatics Engineering
University of Calgary
2500 University Drive N.W., Calgary, Alberta, T2N 1N4, Canada
e-mail: bajrachs@ucalgary.ca

Received: 16 January 2005/Accepted: 7 June 2005

Abstract: The main theme of this paper is to study two important aspects of precise geoid determination using Helmert's second method of condensation. This work illustrates via numerical investigations the importance of using actual density information of topographical bulk and the effects that different gravimetric reductions have on gravity interpolation in Helmert geoid computational process, in addition to the commonly used Bouguer scheme. A rugged area in the Canadian Rockies bounded by latitude between 49°N and 54°N and longitude between 236°E and 246°E is selected to carry out numerical investigations. The lateral density information is used in all steps of the Helmert geoid computational process. The Bouguer and residual terrain modelling (RTM) topographic reductions, the Rudzki inversion scheme, and the topographic-isostatic reductions of Pratt-Hayford (PH) and Airy-Heiskanen (AH) are used for gravity interpolation. Results show that the density information should be applied in all steps of the Helmert geoid computational process and that the topographic-isostatic gravimetric reduction schemes like the PH or AH models or the RTM reduction, should be applied for smooth gravity interpolation instead of the commonly used Bouguer reduction scheme for precise Helmert geoid determination.

Keywords: Geoid, gravity interpolation, actual density, terrain reduction

1. Introduction

The actual density information plays an important role in the solution of the geodetic boundary value problem using Stokes's formula. The classical Stokes's solution assumes that there are no masses above the geoid. Different gravimetric reduction schemes exist to treat the topographical masses above the geoid. Realistic density information is required for every gravimetric terrain reduction scheme to effectively and rigorously model the topographical masses above the geoid. Constant density is practically often used due to unavailability of actual crust density information. Real density information, however, is available these days in some parts of the world in the form of a two-dimensional digital density model (DDM). This actual density data should be incorporated to rigorously remove all masses above the geoid before using Stokes's formula. A three-dimensional DDM containing the information on the vertical variation of

density has not yet been available, though it is required to represent the real topographical density distribution of crustal masses. Some studies using actual density information have been recently carried out by Tziavos et al. (1996), Kühtrelber (1998), Huang et al. (2000), Tziavos and Featherstone (2000), Bajracharya et al. (2002), Kuhn (2003). These studies suggest that the effect of actual density information can alter the geoid as much as decimetre and the actual density information is important for precise geoid determination with centimetre accuracy. Tziavos and Featherstone (2000) illustrated the importance of using actual density information in gravity interpolation for precise geoid determination using Helmert's second method of condensation. The geoid computational methodology presented here is different from the one used by Huang et al. (2000). This paper uses the planar approximation of the geoid, free air reduction to transfer gravity points from the topography to the geoid and GPS/levelling geoid solution for the validation of total gravimetric geoid model. In this paper, a two-dimensional DDM is applied for geoid determination using Helmert's second scheme of condensation. There are three steps in the computational process of Helmert geoid determination, where the lateral density information are applied: (i) computation of Bouguer anomalies which is commonly used in interpolation of free-air anomalies; (ii) computation of terrain correction, which represents the direct topographical effect on gravity and is equal to the difference between the attraction of topography evaluated on the topographical surface and the attraction of condensed masses evaluated on the geoid; and (iii) computation of indirect topographical effects on geoid. It should be noted that the use of lateral density variation assumes that the horizontal variation in density of topographical bulk continues vertically down to the geoid. The GPS/levelling geoid model is generally used for the validation of gravimetric geoid solution. The GPS/levelling geoid solution based on constant density is used in this paper though that using the actual density information is required for rigorous and fair comparison with gravimetric geoid solution using variable density.

The interpolation of free-air anomalies is another important issue using this reduction method. Though Helmert's second method of condensation is mostly used in practice as the mass reduction technique, Helmert anomalies based on this method are very rough (e.g. Li et al., 1995; Omang and Forsberg, 2000; Bajracharya, 2003; Heck, 2003; Kuhn, 2003). For this reason, the Bouguer reduction is commonly used in practice for the interpolation of free-air anomalies. The main principle of using this indirect method for the interpolation is that all the topographical masses above the geoid are removed before gridding free-air anomalies and then the corresponding Bouguer effect is added back to the gridded gravity values. In this paper, different reduction schemes are used for interpolation. The Bouguer and RTM topographic reductions, the Rudzki inversion scheme, and the topographic-isostatic reductions of PH and AH are used to remove terrain effects before gridding free-air anomalies, and then their corresponding topographic or topographic-isostatic or inverted masses are restored to produce gridded FA anomalies.

2. Computational formulae

Helmert gravimetric geoid determination is carried out using remove-compute-restore (RCR) technique in this investigation. In a remove step, the reduced gravity anomalies according to Helmert's second method of condensation can be expressed as:

$$\Delta g = \Delta g_F + c + \Delta g_{ind} - \Delta g_{GM} \tag{1}$$

where Δg_F is the free-air (FA) anomaly, c (terrain correction) is the direct topographical effect on gravity in Helmert's second method of condensation, Δg_{ind} is the indirect effect on gravity (which reduces gravity anomaly from the co-geoid to the geoid), and Δg_{GM} is the reference gravity anomaly from a geopotential model (which represents the low frequency part of the gravity signal).

The main objective of second investigation of this paper is to study the differences between using different gravimetric terrain schemes for interpolating Δg_F in (1) in addition to usual Bouguer reduction method. The procedure for interpolation of free-air anomalies using different gravimetric reduction schemes is given in subsections. In this study, the Helmert geoid models obtained from using the Bouguer, Airy-Heiskanen, Pratt-Hayford, Rudzki, and RTM gravimetric reductions for gravity interpolation are named Bouguer-Helmert, Airy-Helmert, Pratt-Helmert, Rudzki-Helmert, and RTM-Helmert, respectively, and the one obtained from directly interpolated FA anomalies is termed direct-Helmert. This section presents the mathematical formulations for Helmert gravimetric geoid determination.

The commonly used normal gravity gradient of 0.3086 mGal/m is applied for the computation of free-air anomalies Δg_F (in equation (1)). The terrain correction, c, which is equal to the difference between the attraction of the topography evaluated on the surface of the topography and the attraction due to the condensed masses evaluated on the geoid, in (1) is given by (Heiskanen and Moritz, 1967)

$$c = G \iint_E \int_h^{h_p} \frac{\rho(h_p - z)}{s^3(x_p - x, y_p - y, h_p - z)} dxdydz \tag{2}$$

where G is the universal gravitational constant, h_p and h are the height of the computation point and running point respectively, $(x_p, y_p,)$ and (x, y) are the rectangular coordinates of the computation and running point, E is the area, ρ is the density of topographical masses, and s is the distance between computation and running point. The terrain correction algorithm (when the integral (2) is expanded into binomial series) is evaluated by two-dimensional fast Fourier transform (FFT) for mass prism model. The details on algorithms using digital terrain model (DTM) and constant density or digital density model (DDM) can be found in Tziavos et al. (1996) and Li et al. (2000). The indirect effect on gravity, Δg_{ind}, in (1) can be expressed as (Sideris and She, 1995):

$$\Delta g_{ind} \approx \frac{2\pi G\rho h^2}{R} \tag{3}$$

where R is Earth's mean radius. The reference gravity field is computed from the EGM96 geopotential model complete to degree and order 360. In spherical approximation, the reference gravity anomaly at latitude φ_p and longitude λ_p is expressed by (Heiskanen and Moritz, 1967)

$$\Delta g_{GM} = \frac{GM}{R^2} \sum_{n=2}^{n_{max}} (n-1) \sum_{m=0}^{n} [\bar{C}_{nm} \cos m\lambda_p + \bar{S}_{nm} \sin m\lambda_p] P_{nm}(\sin \varphi_p) \tag{4}$$

where $\bar{C}_{nm}$ and $\bar{S}_{nm}$ are the fully normalized spherical harmonic coefficients of the anomalous potential, and P_{nm} is the fully normalized associated Legendre function.

The total geoid undulation obtained from the restore step can be formulated as:

$$N = N_{\Delta g} + N_{ind} + N_{GM} \tag{5}$$

where $N_{\Delta g}$, N_{ind} and N_{GM} denote residual geoid undulation, the indirect effect on the geoid and the long wavelength part of the geoid, respectively. Stokes's integral formula with the rigorous spherical kernel by the one-dimensional fast Fourier transform (1D-FFT) algorithm is used in this paper (Haagmans et al., 1993). The formula for the computation of N_{GM} is given in Heiskanen and Moritz (1967). The indirect effect on geoid, in (5), for Helmert's second scheme of condensation can be expressed as (Wichiencharoen, 1982):

$$N_{ind} = -\frac{\pi G\rho}{\gamma} h_p^2 - \frac{G\rho}{6\gamma} \iint_E \frac{h^3 - h_p^3}{s_o^3} dxdy \tag{6}$$

where γ is the normal gravity and $s_o = [(x - x_p)^2 + (y - y_p)^2]^{1/2}$.

2.1. Bouguer reduction

The Bouguer reduction is a common method to interpolate free-air anomalies in the computation of Helmert geoid. The Bouguer reduction in this paper represents only the removal of topographical masses contained in the Bouguer plate without taking rough part of the topography into account and can be mathematically expressed by the following formula:

$$\Delta g_B = \Delta g_F - 2\pi G\rho h_p \tag{7}$$

After gridding Bouguer anomalies (which are computed at randomly distributed gravity points using equation (7)), they are converted into gridded free-air anomalies using the following formula:

$$\Delta g_F(grid) = \Delta g_B(grid) + 2\pi G\rho h_{DEM} \tag{8}$$

The second term in equation (8) is Bouguer plate correction using the cell height (h_{DEM}).

2.2. Pratt-Hayford topographic-isostatic reduction

The Pratt-Hayford reduction method is one of the topographic-isostatic reduction schemes used in physical geodesy. According to this mass reduction scheme, the density underneath high mountains is uniformly smaller than that under moderate lands. The compensation

starts from directly under the mountains and reaches down to a compensation depth D, where isostatic equilibrium exists. The density contrast between standard crustal density and the actual density in this model can be given as (Heiskanen and Moritz, 1967)

$$\Delta\rho = \rho - \rho_r = \frac{h}{D+h}\rho \text{ (for land)}; \quad \Delta\rho = \rho - \rho_r = \frac{h_o}{D-h_o}(\rho - \rho_w) \text{ (for ocean)} \tag{9}$$

The compensation depth D is assumed equal to 100 km. The normal or standard density value is taken equal to 2.67 g/cm^3. ρ_r is the actual crust density. h_o and ρ_w are the depth of the ocean and the density of the water, respectively. The Pratt-Hayford gravity anomalies can be mathematically expressed as

$$\Delta g_{Pratt} = \Delta g_F - A_{Pratt} \tag{10}$$

where A_{Pratt} is the direct topographical effect in the PH model, which can be regarded as the attraction change due to the topographical masses above the geoid and compensated masses below the geoid, which lie within the depth of compensation and can be expressed as follows:

$$A_{Pratt} = G\rho\iiint_{E0}^{h}\frac{(h_p - z)}{s^3(x_p - x, y_p - y, h_p - z)}dxdydz - G\Delta\rho\iiint_{E\cdot D}^{0}\frac{(h_p - z)}{s^3(x_p - x, y_p - y, h_p - z)}dxdydz \tag{11}$$

where the first and second terms represent the attraction of the topographical masses and the compensated masses according to PH model, respectively. The integrals in (11) are evaluated by the numerical integration using standard prism method (Nagy, 1966)

$$A = G\rho \,|||\, x\ln(y + r) + y\ln(x + r) - z\arctan\frac{xy}{zr}\Big|_{x_1}^{x_2}\Big|_{y_1}^{y_2}\Big|_{z_1}^{z_2} \tag{12}$$

where coordinates x_1, x_2, y_1, y_2, z_1 and z_2 represent the corners of a prism. The Pratt-Hayford anomalies, obtained in gravity stations after applying computed values of attraction change from equation (11) to equation (10), are gridded and they are converted into gridded free-air anomalies using the following formula:

$$\Delta g_F(grid) = \Delta g_{Pratt}(grid) + A_{Pratt}(h_{DEM}) \tag{13}$$

The second term in above equation represents the correction to the direct topographical effect on gravity according to PH scheme.

2.3. Airy-Heiskanen topographic-isostatic reduction

The AH model is based on the principle that mountains are floating on material of higher density forming roots under mountains and anti-roots under the oceans. The density contrast

between the Earth's crust and the upper mantle in the AH model can be expressed as (Heiskanen and Moritz, 1967)

$$\Delta\rho = \rho_m - \rho = \frac{h\rho}{t} \text{ (for land)}; \qquad \Delta\rho = \rho_m - \rho = \frac{\rho - \rho_w}{t'} h_o \text{ (for ocean)} \tag{14}$$

where t and t' represent the thickness of root and anti-root, and ρ_m is density of upper mantle, which is equal to 3.27 g/cm^3. h_o and ρ_w are the depth of the ocean and the density of the water, respectively. The normal crust thickness, T, is assumed to be 30 km. The Airy-Heiskanen gravity anomalies are formulated as

$$\Delta g_{Airy} = \Delta g_F - A_{Airy} \tag{15}$$

The second term in equation (15) is the direct topographical effect due to AH topographic-isostatic scheme, which is the difference in the attraction between topographical masses and their compensating masses within the depth of the root or anti-root and can be given by

$$A_{Airy} = G\rho \iiint_{E\,0}^{h} \frac{(h_p - z)}{s^3(x_p - x,\, y_p - y,\, h_p - z)}\, dxdydz - G\Delta\rho \iint_{E\,-T-t}^{0} \int \frac{(h_p - z)}{s^3(x_p - x,\, y_p - y,\, h_p - z)}\, dxdydz \tag{16}$$

The above integrals are evaluated by the equation (12). The gridded Pratt-Hayford anomalies obtained using equations (15) and (16) are converted to free-air anomalies using the following formula:

$$\Delta g_F(grid) = \Delta g_{Airy}(grid) + A_{Airy}(h_{DEM}) \tag{17}$$

The term, A_{Airy}, is a correction for the direct topographical effect on gravity according to AH mass reduction technique.

2.4. Rudzki inversion gravimetric scheme

The topographical masses above the geoid are inverted into its interior in Rudzki reduction scheme. The Rudzki anomalies are given as

$$\Delta g_{Rudzki} = \Delta g_F - A_{Rudzki} \tag{18}$$

A_{Rudzki}, which is equal to the difference between the gravitational attraction due to all topographical masses above the geoid and that due to the mirrored topographical masses inside the geoid in Rudzki's scheme, can be expressed as

$$A_{Rudzki} = G\rho \iiint_{E\,0}^{h} \frac{(h_p - z)}{s^3(x_p - x,\, y_p - y,\, h_p - z)}\, dxdydz - G\rho' \iint_{E\,-h'}^{0} \int \frac{(h_p - z)}{s^3(x_p - x,\, y_p - y,\, h_p - z)}\, dxdydz \tag{19}$$

where ρ' and h' are the density and depth of inverted masses which are equal to the density and height of the topographical masses in planar approximation (Heiskanen and Moritz, 1967; Bajracharya, 2003), respectively. The integrals in equation (19) are evaluated by the prism formula (12). The gridded Rudzki anomalies obtained using equations (18) and (19) are used to obtain free-air anomalies after applying the correction term of direct Rudzki terrain effect (A_{Rudzki}) as follows:

$$\Delta g_F(grid) = \Delta g_{Rudzki}(grid) + A_{Rudzki}(h_{DEM}) \tag{20}$$

2.5. Residual terrain model

The topographical masses above the reference surface, which is defined by low pass filtering of local terrain heights, are removed and masses are filled up below this surface in the RTM gravimetric reduction scheme (Forsberg, 1984). The RTM anomalies are expressed as

$$\Delta g_{RTM} = \Delta g_F - A_{RTM} \tag{21}$$

A_{RTM}, the attraction change due to the difference between the gravitational attraction of all topographical masses above the geoid and that due to the referenced masses, can be expressed as

$$A_{RTM} = G\rho \iiint_{E\,0}^{h} \frac{(h_p - z)}{s^3(x_p - x, y_p - y, h_p - z)} dxdydz - G\rho \iiint_{E\;0}^{h_{ref}} \frac{(h_p - z)}{s^3(x_p - x, y_p - y, h_p - z)} dxdydz \tag{22}$$

where h_{ref} represents the height of reference surface.

The direct RTM topographical effect in equation (22) can be computed using rectangular prisms given by formula (12). The gridded RTM anomalies obtained from the equation (21) are transferred to gridded free-air anomalies using the following formula

$$\Delta g_F(grid) = \Delta g_{RTM}(grid) + A_{RTM}(h_{DEM}) \tag{23}$$

where A_{RTM} represents a correction term of direct RTM terrain effect using the cell height.

In the first part of this investigation, the Bouguer reduction described in section (2.1) is used for interpolating free-air anomalies for the study of density effects on Helmert geoid solution. The actual density information is incorporated in equations (2), (6), (7), and (8) for the computation of terrain correction, indirect effects on gravity, Bouguer anomalies, and Bouguer correction, respectively.

For the study of interpolation effects (second part of investigation), the gridded free-air anomalies obtained using equations (8), (13), (17), (20), and (23) are applied in equation (1) to get a set of reduced Helmert anomalies, which is used to obtain different gravimetric Helmert solutions as described from section (2.1) to section (2.5). This part of investigation is carried out using constant density.

3. Numerical tests

A test area in this investigation covers the part of Canadian Rockies bounded by latitude between 49°N and 54°N and longitude between 236°E and 246°E. The test area and all data sets used are same for both investigations, except for the DTM grid resolution. There are 9477 gravity measurements available, the coverage of which is given in Fig. 1.

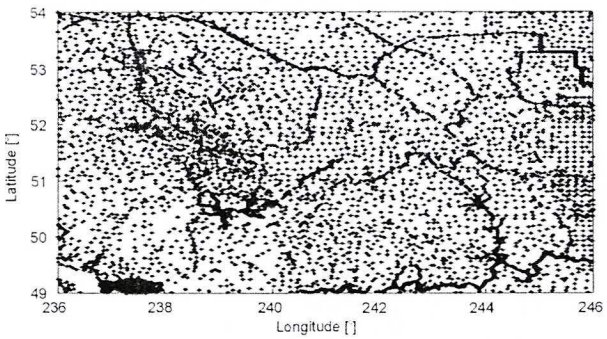

Fig. 1. Distribution of gravity points in the test area

The constant density of topographical masses is assumed to be 2.67 g/cm^3. A digital terrain model with 15″ grid resolution is used for the study of gravity interpolation effect on Helmert geoid determination. The grid resolution of two-dimensional DDM available for this study is 30″ and thus a 30″ grid spacing of DTM and DDM is used for the study of density effects on Helmert's second technique of condensation. The topography of the test area is shown in Fig. 2.

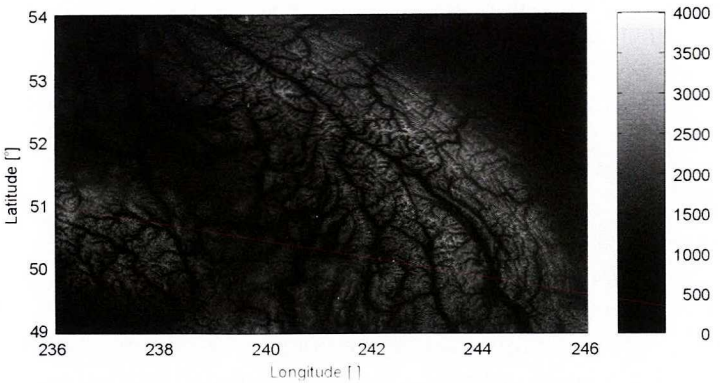

Fig. 2. Digital terrain model in the test area [m]

The topography has a maximum elevation of 3937 m with a standard deviation of 543 m and a mean elevation of 1396 m. A radius of 300 km is used around the computation point to compute the gravitational attraction of the topography, the attraction of the compensating masses, and the attraction of the inverted masses in the second test. The long wavelength part of the gravity field is computed from the EGM96 geopotential model

complete to degree and order 360. The compensation depth of 100 km for PH model and the normal crust thickness of 30 km for AH model are assumed to compute the gravitational attraction of compensating masses according to these models. The density contrast between the crustal masses and the upper mantle is taken equal to 0.6 g/cm^3. Figure 3 shows large contrasts in the topographic density of the test area, with maximum and minimum values of 2.98 g/cm^3 and 2.49 g/cm^3, respectively.

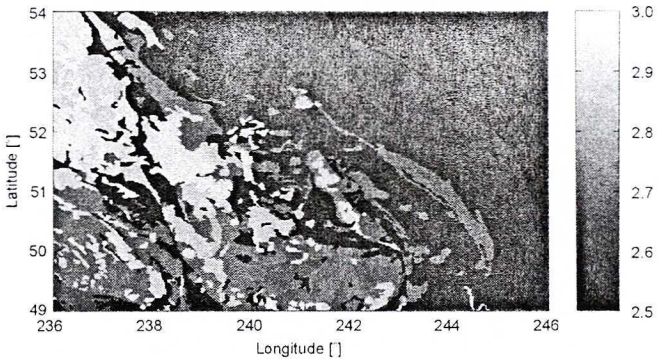

Fig. 3. Digital density model in the test area [g/cm^3]

The GPS/levelling data set is used to assess the precision of Helmert gravimetric geoid solutions for both studies. There are altogether 258 GPS benchmarks available for this test area and their distribution is given in Fig. 4.

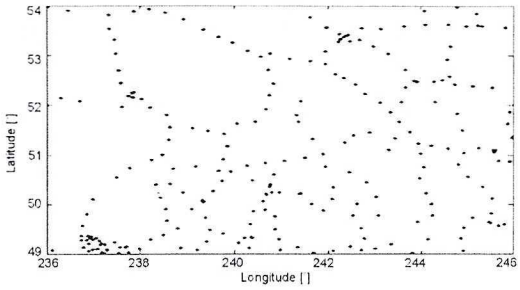

Fig. 4. Distribution of GPS/levelling points in the test area

3.1. Density effects

The information on density, which is available as a two-dimensional digital density model for the test area, is incorporated in all steps of the geoid computational process. The actual density information is used in the computation of Bouguer anomalies (which are used for the interpolation of free-air anomalies), in the computation of terrain correction, and in the computation of the indirect effect on geoid for this mass reduction scheme.

The topographical density effect on Helmert anomalies includes both the direct topographical density effect (DTDE) and the density interpolation effect (DIE) on gravity (given in Table 1).

Table 1. The statistics of DTDE and the density effect on Bouguer and Helmert anomalies [mGal]

Gravimetric quantities	Max	Min	Mean	Std
DTDE	10.87	−4.91	0.13	0.36
Bouguer anomalies	29.08	−28.27	−4.05	5.54
Helmert anomalies	32.75	−41.91	−4.01	7.24

The magnitude of density effect on Helmert anomalies (74.7 mGal in range), in which DTDE (15.8 mGal) contributes 21% in range and the rest is contributed by DIE, clearly exhibits the importance of using density information in gravity interpolation. The variable density has a large effect in the modelling of topographical masses using Bouguer scheme, which is used in the interpolation procedure of Helmert anomalies. The DTDE, shown in Fig. 5, is correlated both with topography and topographical density of test area.

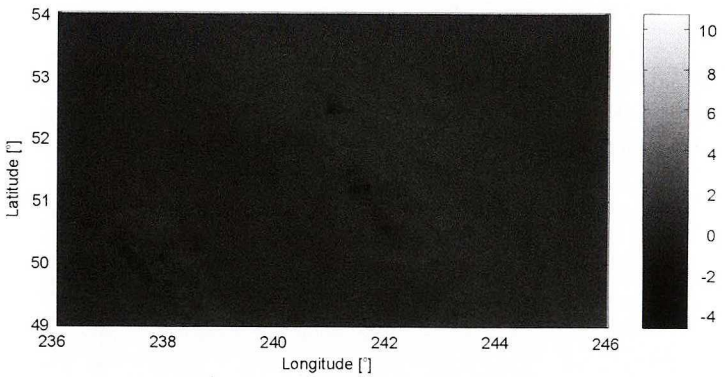

Fig. 5. DTDE on gravity [mGal]

The DTDE, indirect density effect (IDE), DIE, and total density effect (direct, indirect and interpolation effects) on geoid undulation are shown in Table 2.

Table 2. The statistics of DTDE, IDE, DIE, and total density effect on geoid [m]

Effects on geoid	Max	Min	Mean	Std
DTDE	0.11	−0.01	0.05	0.02
IDE	0.05	−0.03	0.00	0.01
DIE	−0.41	−2.56	−1.51	0.48
Total density effect	−0.41	−2.52	−1.47	0.48

The DTDE and IDE can alter the geoid as much as 10 cm and 5 cm, respectively (presented in Table 2). These values show that the incorporation of actual density information in the computation of direct topographical effect and indirect effect is crucial in centimetre geoid determination. The IDE on geoid, shown in Fig. 6, is correlated with the topography and topographical density of Canadian Rockies. Moreover, the DIE on geoid, shown in Table 2, is most prominent one compared to DTDE and IDE. It can affect the accuracy of Helmert geoid as much as 2.56 m. This value exhibits the significance of using actual density information in precise Helmert geoid determination, especially in the process of interpolation. It is interesting to note that DIE (shown in Table 2) on geoid is as big as the total terrain effect on geoid in the range and mean values (Bajracharya et al., 2002).

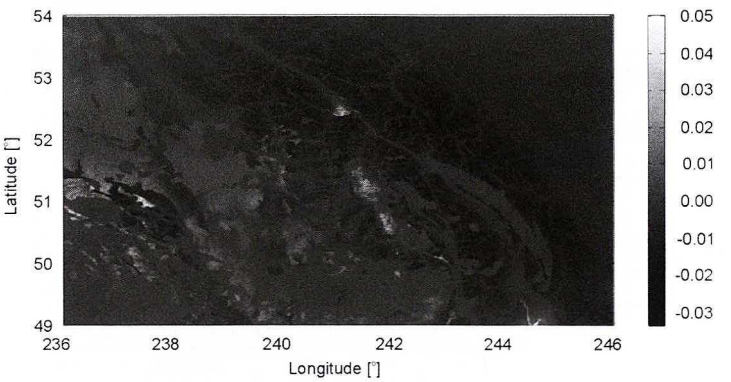

Fig. 6. IDE on geoid [mGal]

The statistics of the differences between Helmert gravimetric geoid solutions using constant and variable density with the GPS/levelling geoid is shown in Table 3.

T a b l e 3. The statistics of difference between Helmert gravimetric geoid solutions using constant and variable density with GPS/levelling geoid (before and after fit) [m]

Density	Max	Min	Mean	Std
Constant (before fit)	−0.28	−3.04	−1.61	0.56
Variable (before fit)	0.55	−1.70	−0.15	0.34
Constant (after fit)	0.54	−1.27	0.00	0.25
Variable (after fit)	0.69	−0.77	−0.00	0.25

The Helmert gravimetric geoid solution incorporating actual density information exhibits better results (by 40% in terms of standard deviation and 20% in range) than the one using constant density. However, the density effect is eliminated and the standard deviation becomes same for both, when a four-parameter trend surface is applied to fit Helmert gravimetric geoid solutions to the GPS/levelling. The range using DDM, though, is still smaller.

3.2. Interpolation effects

The procedure for computing the Helmert geoid in this study is the same one applied in previous investigation. The results presented here come from the difference of using different gravimetric reduction methods for gridding free-air anomalies instead of using just a simple Bouguer scheme. The constant density is applied in this part of investigation.

The most important properties of gravity anomalies for their interpolation are (i) they should be smooth and (ii) they should not depend on elevation. PH and AH anomalies are the best anomalies for gravity interpolation in the test area as we can see from the statistics of gravity anomalies and their correlation coefficients with topography, given in Table 4.

Table 4. The statistics of gravity anomalies [mGal] and their correlation coefficients with topography

Reduction scheme	Max	Min	Mean	Std	Corr. coeff.
Free-air	166.38	−183.58	−22.39	50.71	0.80
Refined Bouguer	−5.52	−212.87	−110.08	43.62	−0.75
Helmert	248.67	−156.21	−14.86	58.76	0.85
AH	54.09	−133.97	−24.95	19.16	0.14
PH	49.68	−118.87	−29.62	18.28	0.07
RTM	116.67	−91.57	−0.58	24.00	0.65
Rudzki	124.71	−121.56	−17.39	35.97	0.84

The correlation trends of gravity anomalies with topography, given in Fig. 7, also shows that PH and AH anomalies are least dependent on topography. The RTM anomalies suit better than commonly used Bouguer anomalies for gravity interpolation in the test area since they are smoother in terms of standard deviation and less dependent on topography.

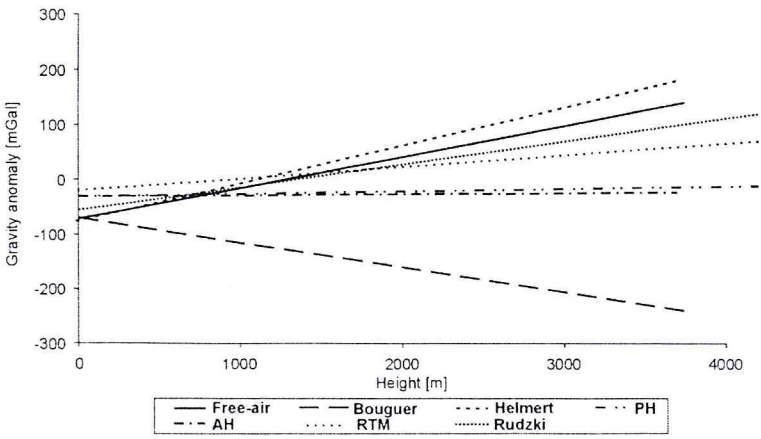

Fig. 7. Correlation trends between gravity anomalies and topography

The different sets of free-air anomalies are obtained using different mass reduction schemes for gridding. Their statistics, given in Table 5, show that free-air anomalies using any gravimetric reduction for interpolating become smoother in terms of standard deviation and range than those using directly computed free-air anomalies.

T a b l e 5. The statistics of free-air anomalies using different mass reduction schemes for interpolating free-air anomalies [mGal]

Reduction scheme used for gridding	Max	Min	Mean	Std
Direct (free-air)	166.38	−183.58	−22.39	50.71
Bouguer	160.24	−176.69	−2.31	45.67
Airy Heiskanen	158.37	−169.71	3.45	47.85
Pratt-Hayford	158.83	−162.65	3.57	47.66
RTM	159.50	−163.41	4.61	47.82
Rudzki	154.12	−151.36	3.03	44.91

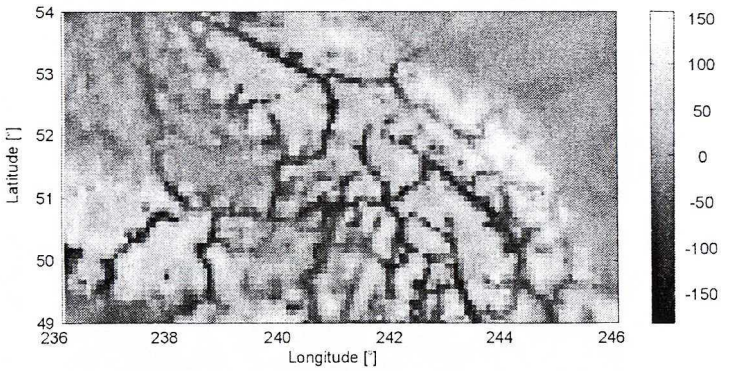

Fig. 8. Free-air anomalies (directly interpolated) [mGal]

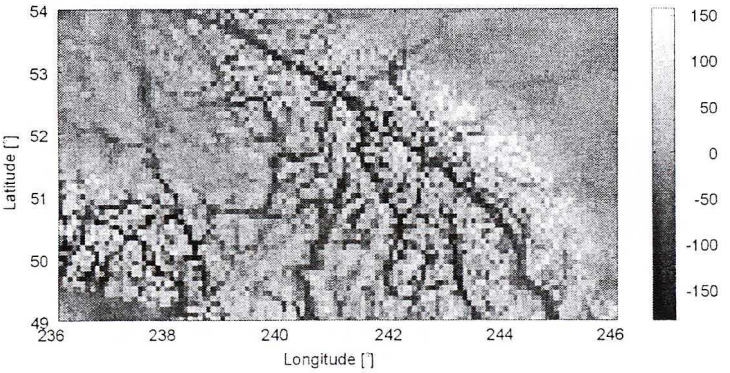

Fig. 9. Free-air anomalies (interpolated using Bouguer scheme) [mGal]

Figures 8 and 9 show the directly interpolated free-air anomalies and those obtained from using Bouguer reduction for interpolation, respectively.

The difference (presented in Table 6) can reach between 157 mGal and 229 mGal in maximum value and 31 mGal and 43 mGal in standard deviation depending on the reduction scheme chosen. This difference (shown in Fig. 10 for Bouguer scheme) looks similar for all sets of free air anomalies and is correlated with the topography of Canadian Rockies.

T a b l e 6. Difference between FA anomalies directly interpolated and after applying different mass reduction schemes for interpolation [mGal]

Reduction scheme	Max	Min	Mean	Std
Direct-refined Bouguer	228.57	−216.42	13.37	43.12
Direct-Airy	214.32	−204.65	7.61	38.23
Direct-Pratt	208.41	−200.61	7.49	37.71
Direct-RTM	217.37	−203.20	6.45	37.93
Direct-Rudzki	157.62	−139.44	8.03	31.29

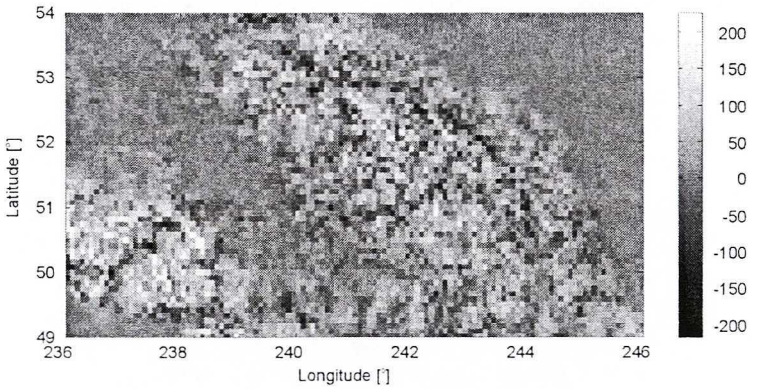

Fig. 10. Difference between free-air anomalies directly interpolated and interpolated using Bouguer scheme [mGal]

T a b l e 7. The statistics of difference of Helmert geoid models using different mass reduction schemes for interpolation [m]

Reduction scheme	Max	Min	Mean	Std
Direct-refined Bouguer	9.00	2.18	4.62	1.29
Direct-Airy	5.83	0.91	2.55	0.81
Direct-Pratt	5.72	0.91	2.51	0.80
Direct-RTM	5.56	0.52	2.23	0.83
Direct-Rudzki	5.51	1.24	2.79	0.84

The Helmert geoid models using different gravimetric reduction techniques for gridding free-air anomalies are computed. The differences between the direct-Helmert geoid and the other Helmert geoid models (given in Table 7) can reach between 5 m and 9 m in maximum value depending on the reduction method used.

The difference is correlated with the topography as shown in Fig. 11 for Bouguer reduction. These results suggest that one should not use directly interpolated free-air anomalies for Helmert geoid determination.

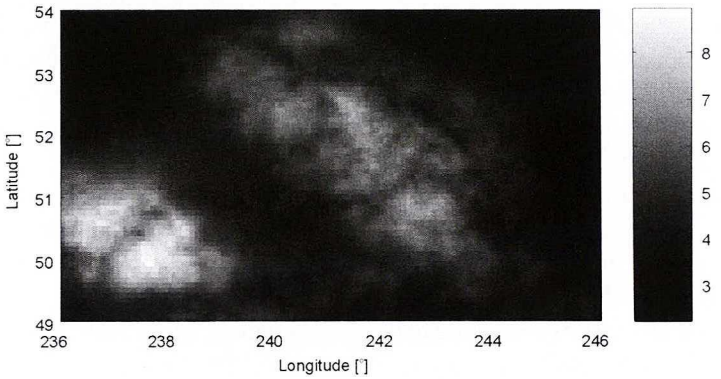

Fig. 11. Difference between directly interpolated Helmert geoid and Bouguer-Helmert geoid [m]

T a b l e 8. The statistics of difference between different Helmert geoid models and GPS/levelling geoid solution [m]

Helmert geoid	Max	Min	Mean	Std
Direct-Helmert	5.20 (2.33)	1.52 (−1.12)	2.62 (0.00)	0.55 (0.51)
Bouguer-Helmert	−0.24 (0.60)	−3.11 (−1.34)	−1.62 (0.00)	0.55 (0.25)
AH-Helmert	0.86 (0.56)	−0.34 (−0.56)	0.34 (0.00)	0.21 (0.18)
PH-Helmert	0.88 (0.55)	−0.32 (−0.55)	0.38 (0.00)	0.21 (0.18)
RTM-Helmert	1.23 (0.56)	−0.07 (−0.56)	0.66 (0.00)	0.23 (0.19)
Rudzki-Helmert	0.78 (0.61)	−0.86 (−0.56)	0.06 (0.00)	0.31 (0.18)

The statistics of the differences between different Helmert geoid models and the GPS/levelling geoid solution are given in Table 8. The results show that the AH-Helmert, PH-Helmert, and RTM-Helmert geoid models demonstrate better fit with GPS/levelling geoid of the test area before (by 58% in terms of standard deviation) and after (by 28% in terms of standard deviation) fit than the Bouguer-Helmert. Also, the range of these geoid

models is smaller compared to that of Bouguer-Helmert both before and after fit. It is interesting to note comparing between Rudzki-Helmert and Bouguer-Helmert that Rudzki anomalies, which are highly correlated with topography but smoother than Bouguer anomalies in terms of standard deviation, work better for interpolation than Bouguer anomalies.

4. Conclusions

This paper investigated two important aspects of precise Helmert geoid determination. The first study of this paper has illustrated the importance of using actual crust density information in all steps of Helmert geoid determination. The DIE on geoid is much larger than the sum of DDE and IDE on geoid. The total density effect on Helmert geoid can be as big as total terrain effect on geoid. The variable density information (if available) should be incorporated in the computation of Bouguer anomalies if it is chosen for gravity interpolation. The total density effect will become bigger if the higher resolution of DDM (which is currently not available) and DTM are used. Helmert geoid determination incorporating actual Earth crust density information in all steps of its computational process shows better results compared to the GPS/levelling geoid of the test area in terms of range and standard deviation (34 cm) than using constant density (56 cm) before fit. The actual density information should be used (if available) in precise geoid determination in high mountains, especially where large contrast in topographical density exists. As stated earlier, the GPS levelling geoid solution based on variable density information (if available) should be used for the rigorous validation of gravimetric geoid solution using variable density.

A very important conclusion can be drawn from the second study of this paper, namely, that the use of a proper gravimetric terrain reduction scheme for the interpolation of free-air gravity anomalies plays a key role in precise Helmert geoid computation, especially in areas of rugged topography. The AH-Helmert, PH-Helmert, and RTM-Helmert, which use smoother and less correlated gravity anomalies than Bouguer anomalies, possess better statistics (42% in range and 28% in standard deviation) than Bouguer-Helmert geoid. The commonly used Bouguer reduction scheme should be thus replaced by the topographic-isostatic gravimetric reduction schemes like the AH or PH model, or by the RTM topographic reduction method for gravity interpolation in the context of precise Helmert geoid determination, especially in rough terrain.

Acknowledgements

This research has been supported by grants to the second author from the Geomatics for Informed Decisions (GEOIDE) Network of Centers of Excellence (NCE) and the Natural Sciences and Engineering Research Council of Canada. We are grateful to an anonymous reviewer for his constructive comments that have helped to improve the quality of this manuscript.

References

Bajracharya S., Kotsakis C., Sideris M.G., (2002): *Aliasing effects on terrain correction computation*, International Geoid Service, Bulletin No 12, April 2002.

Bajracharya S., (2003): *Terrain effects on geoid determination*, MSc. Thesis, University of Calgary, Department of Geomatics Engineering, Report No 20181.

Forsberg R., (1984): *A study of terrain reductions, density anomalies and geophysical inversion methods in gravity field modelling*, OSU Report No 355, Department of Geodetic Science and Surveying, The Ohio State University, Columbus, Ohio.

Haagmans R., de Min E., van Gelderen M., (1993): *Fast evaluation of convolution integrals on the sphere using 1D FFT and a comparison with existing methods for Stokes' integral*, Manuscripta Geodaetica, Vol. 18, pp. 227-241.

Heck B., (2003): *On Helmert's methods of condensation*, Journal of Geodesy, Vol. 77, No 3-4, pp. 155-170.

Heiskanen W.A., Moritz H., (1967): *Physical geodesy*, W.H. Freeman and Company, San Francisco.

Huang J., Vanicek P., Pagiatakis S.D., Brink W., (2000): *Effect of topographical density on geoid in the Canadian Rocky Mountains*, Journal of Geodesy, Vol. 74, No 11-12, pp. 805-815.

Kühtrelber N., (1998): *Precise geoid determination using a density variation model*, Physics and chemistry of the Earth, Vol. 23, No 1, pp. 59-63.

Kuhn M., (2003): *Geoid determination with density hypotheses from isostatic models and geological information*, Journal of Geodesy, Vol. 77, No 1-2, pp. 50-65.

Li Y.C., Sideris M.G., Schwarz K.P., (2000): *Unified terrain correction formulas for vector gravity measurements*, PINSA, 66, A, No 5, September 2000, pp. 521-535.

Li Y.C., Sideris M.G., Schwarz K.P., (1995): *A numerical investigation on height anomaly prediction in mountainous areas*, Bulletin Géodésique, Vol. 69, pp. 143-156.

Nagy D., (1966): *The prism method for terrain corrections using digital computers*, Pure Applied Geophysics, Vol. 63, pp. 31-39.

Omang O.C.D., Forsberg R., (2000): *How to handle topography in practical geoid determination: three examples*, Journal of Geodesy, Vol. 74, No 6, pp. 458-466.

Sideris M.G., She B.B., (1995): *A new, high resolution geoids for Canada and part of the US by the 1D-FFT method*, Bulletin Géodésique, Vol. 69, pp. 92-108.

Tziavos I.N., Featherstone W.E., (2000): *First results of using digital density data in gravimetric geoid computation in Australia*, IAG Symposia, Vol. 123, M.G. Sideris (ed.), GGG2000, ©Springer Verlag Berlin Heidelberg (2001), pp. 335-340.

Tziavos I.N., Sideris M.G., Sünkel H., (1996): *The effect of surface density variation on terrain modelling – A case study in Austria*, Proceedings, EGS Society General Assembly, The Hague, The Netherlands, May 1996, Report of the Finnish Geodetic Institute.

Wichiencharoen C., (1982): *The indirect effects on the computation of geoid undulations*, OSU Report No 336, Department of Geodetic Science and Surveying, The Ohio State University, Columbus, Ohio.

Efekty interpolacji gęstości i przyspieszenia siły ciężkości na wyznaczenie geoidy Helmerta

Sujan Bajracharya, Michael G. Sideris

Wydział Inżynierii Geomatycznej, Uniwersytet w Calgary,
2500 University Drive N.W., Calgary, Alberta, T2N 1N4, Kanada
e-mail: bajrachs@ucalgary.ca

Streszczenie

Tematem pracy jest badanie dwóch istotnych aspektów wyznaczania geoidy przy zastosowaniu drugiej metody kondensacji Helmerta. Przy użyciu badań numerycznych zilustrowane zostało w pracy znaczenie wykorzystania

aktualnej informacji o gęstości topografii terenu oraz efektów różnych rodzajów redukcji grawimetrycznych na interpolację przyspieszenia siły ciężkości w procesie obliczania geoidy Helmerta, uzupełniających powszechnie stosowaną procedurę opartą na anomaliach Bouguera. Do przeprowadzenia testów numerycznych wybrano silnie pofałdowany obszar w kanadyjskiej części Gór Skalistych pomiędzy równoleżnikami 49°N i 54°N i pomiędzy południkami 236°E i 246°E. We wszystkich krokach procesu obliczania geoidy Helmerta używano informacji o rozkładzie gęstości warstwy topografii nad poziomem morza. Do interpolacji przyspieszenia siły ciężkości wykorzystano anomalie Bouguera, redukcje topograficzne w oparciu o residualny model terenu (RTM), redukcje Rudzkiego, redukcje topograficzno-izostatyczne Pratta-Hayforda (PH) i Airy-Heiskanena (AH). Uzyskane wyniki wskazują na to, że informacja o gęstości topografii powinna być używana we wszystkich krokach procesu obliczania geoidy Helmerta oraz, że topograficzno-izostatyczna redukcja grawimetryczna, taka jak PH, AH lub RTM, wygładzająca interpolację przyspieszenia siły ciężkości powinna być stosowana do precyzyjnego wyznaczania geoidy Helmerta zamiast powszechnie stosowanej metody opartej na anomaliach Bouguera.